Mapping post-fire monthly erosion rates at the catchment scale using emphirical models implemented in GIS. A case study in Northern Italy

Metadata of the chapter that will be visualized in SpringerLink

Book Title	Progress in Landslide Research and Technology, Volume 1 Issue 1, 2022	
Series Title		
Chapter Title	Mapping Post-fire Monthly Erosion Rates at the Catchment Scale Using Empirical Models Implemented in GIS. A Case Study in Northern Italy	
Copyright Year	2023	
Copyright HolderName	The Author(s)	

Author	Family Name	**Vacha**
	Particle	
	Given Name	**Damiano**
	Prefix	
	Suffix	
	Role	
	Division	Interuniversity Department of Regional and Urban Studies and Planning (DIST)
	Organization	University of Turin
	Address	10125, Turin, Italy
	Email	damiano.vacha@unito.it
Corresponding Author	Family Name	**Mandrone**
	Particle	
	Given Name	**Giuseppe**
	Prefix	
	Suffix	
	Role	
	Division	Interuniversity Department of Regional and Urban Studies and Planning (DIST)
	Organization	University of Turin
	Address	10125, Turin, Italy
	Email	giuseppe.mandrone@unito.it
Author	Family Name	**Morresi**
	Particle	
	Given Name	**Donato**
	Prefix	
	Suffix	
	Role	
	Division	Department of Agricultural, Forest and Food Sciences (DISAFA)
	Organization	University of Turin
	Address	10095, Grugliasco, TO, Italy
	Email	donato.morresi@unito.it
Author	Family Name	**Garbarino**
	Particle	
	Given Name	**Matteo**

Prefix	
Suffix	
Role	
Division	Department of Agricultural, Forest and Food Sciences (DISAFA)
Organization	University of Turin
Address	10095, Grugliasco, TO, Italy
Email	matteo.garbarino@unito.it

Abstract

Post-wildfire geological hazards are an emerging problem for a number of different environments, including areas not typically associated with these events such as the Alpine Region. The risk connected with post-fire processes such as debris-flows and flood-type events threatens people, infrastructures, services and economical activities. Apart from a few examples, such as in the USA and Australia, there is a lack of models available to quantify the increase in susceptibility of the aforementioned phenomena as a result of the modification induced by the wildfires. In this work we test the application of a modified version of the RUSLE, on GIS, to quantify the post-fire erosive phenomena for a case study in the north-western Italian Alps. The results of its application, taking advantage of high-resolution rainfall series and data deriving from field surveys, highlight the marked increase (more than 20 times) in erosion rates, quantified by expressing both the EI (erodibility index), the A (monthly soil loss) and the SL (monthly sediment loss) rise. The months of April, May and June represent the larger share of the total quantities. This is a consequence of the noticeable increase of the EI, which for the post-fire scenario is more than one order of magnitude higher than the pre-fire one.

Keywords (separated by '-'): Wildfires - Erosion - Slope stability - Hazard - Western Alps

Mapping Post-fire Monthly Erosion Rates at the Catchment Scale Using Empirical Models Implemented in GIS. A Case Study in Northern Italy

Damiano Vacha, Giuseppe Mandrone, Donato Morresi, and Matteo Garbarino

Abstract

Post-wildfire geological hazards are an emerging problem for a number of different environments, including areas not typically associated with these events such as the Alpine Region. The risk connected with post-fire processes such as debris-flows and flood-type events threatens people, infrastructures, services and economical activities. Apart from a few examples, such as in the USA and Australia, there is a lack of models available to quantify the increase in susceptibility of the aforementioned phenomena as a result of the modification induced by the wildfires. In this work we test the application of a modified version of the RUSLE, on GIS, to quantify the post-fire erosive phenomena for a case study in the north-western Italian Alps. The results of its application, taking advantage of high-resolution rainfall series and data deriving from field surveys, highlight the marked increase (more than 20 times) in erosion rates, quantified by expressing both the EI (erodibility index), the A (monthly soil loss) and the SL (monthly sediment loss) rise. The months of April, May and June represent the larger share of the total quantities. This is a consequence of the noticeable increase of the EI, which for the post-fire scenario is more than one order of magnitude higher than the pre-fire one.

D. Vacha · G. Mandrone (✉)
Interuniversity Department of Regional and Urban Studies and Planning (DIST), University of Turin, 10125 Turin, Italy
e-mail: giuseppe.mandrone@unito.it

D. Vacha
e-mail: damiano.vacha@unito.it

D. Morresi · M. Garbarino
Department of Agricultural, Forest and Food Sciences (DISAFA), University of Turin, 10095 Grugliasco, TO, Italy
e-mail: donato.morresi@unito.it

M. Garbarino
e-mail: matteo.garbarino@unito.it

Keywords

Wildfires • Erosion • Slope stability • Hazard • Western Alps

1 Introduction

Climate change is having far-reaching effects ranging from unprecedented forest fires, heatwaves, droughts and extreme rainfall events (IPCC 2014a, b). Natural disturbances are thought to experience a further increase in frequency and severity, progressively affecting areas not endangered in the past also due to land use change (Maringer et al. 2016; Mantero et al. 2020). They can occur alone or in combination with each other and cause and/or be followed by secondary hazards, constituting a complex chain of multi-hazards processes also called cascading effect. As an example, forest fires lead to new avalanche-prone slopes, and to a higher risk of rockfall, debris-flow, mudslides, soil erosion and water quality problems. Recent estimates for the Alpine region, forecasting an increased impact of the climate change effects, suggest wildfires and post-wildfire geological hazards to represent a looming issue in the near future (Zumbrunnen et al. 2009; Moreira et al. 2011; Wastl et al. 2012; Arndt et al. 2013, Dupire et al. 2019, Barbero et al. 2019).

Amongst other hydrological hazards, debris-flow and flood-type events represent the most serious concern, as can be seen in the reports and the scientific literature of the regions (USA, Australia) which are facing the problem nowadays (De Graff 2014). The modification of the hydrological properties, due to litter and vegetation removal, ash deposition, alteration of the physical properties of soil and rocks results in an increase of the availability of easily erodible materials on hillslopes and of runoff rates (Moody and Martin 2001; Parise and Cannon 2008, 2012; Staley et al 2017). In fact, rainsplash, sheetflow and rill erosion

K. Sassa et al. (eds.), *Progress in Landslide Research and Technology, Volume 1 Issue 1, 2022*, Progress in Landslide Research and Technology, https://doi.org/10.1007/978-3-031-16898-7_6

increases due to the diminished capacity of rainfall interception by the tree canopies, shrubs and grass. Very soon the surface runoff may concentrate in hollows and low order channels carrying the eroded sediment and entraining the materials deposited in the waterways, eventually exerting a strong erosive action at the expense of the riverbed sediments and causing their "in mass" failure. All of these processes can lead to sediment concentration to levels associated with debris flows (Thang et al. 2019).

Currently, very few models are available for the estimate of the hazard and risk of these phenomena. The USGS preliminary hazard assessment relies on empirical models to assess the likelihood, volume and combined hazard of debris flows for selected watersheds in response to a design storm. These models rely on historical debris–flow occurrence and magnitude data, rainfall storm conditions, terrain and soils information, and burn–severity maps (Staley et al. 2016, 2017). In Australia, the Victorian Department of Sustainability and Environment (DSE) developed an empirical rapid risk assessment procedure for post-fire hydrologic risks, namely debris flows risk, water quality risk and flooding risk. The model, in the early stages of development, is based on available datasets and combines information for terrain, vegetation, rainfall erosivity, burn severity maps and stream network (Sheridan et al. 2009). In other countries, such as the Mediterranean ones, despite an increasing number of hazardous events (Parise and Cannon 2008; Tiranti et al. 2006; Carabella et al. 2019; Esposito et al. 2013, 2017, 2019), no model for the hydro-geomorphic events susceptibility assessment has been implemented or validated extensively. Very few examples of model application can be found in Italy, Greece, Portugal and Spain (Terranova et al. 2009; Fernandez et al. 2010, 2018; Coschignano et al. 2019; Esteves et al. 2013 Rulli et al. 2013; Lanorte et al. 2019; Depountis 2020, Efthimiou 2020). The need to quantify the influence of fires on the propensity for hazardous processes clashes with the fact that, in many regions outside the United States, the scientific community has faced the problem in a consistent way only in recent years and thus the available post-fire event statistics does not allow for a data driven approach. In this study, we focused on the application and validation of a modified version of the RUSLE model (Revised Universal Soil Loss Equation—Wischmeier and Smith 1978) to quantify the post-fire erosive phenomena for a case study in the north-western Italian Alps. In this area, during October 2017, ten wildfires occurred, burning a total area of 10,000 hectares of which 7000 were forests; this value far exceeds the average regional forest burned area (600 ha/year between 2005 and 2013) (Morresi et al. 2022). Season fires in 2017 were favored by the exceptionally dry conditions, high temperatures and the occurrence of several days with hot and dry winds (Arpa Piemonte 2017; Bo et al. 2020). The largest and most severe fire—almost 4000 ha—occurred in the Susa Valley, where fourteen catchments on the left of the Dora Riparia River were involved. Starting from late April 2018 until the early June, several flow events originated from the burned catchments. The larger damages were recorded at the outlet of the Comba delle Foglie, a small drainage basin overhanging the Bussoleno municipality (Vacha et al. 2021). Ground evidence highlighted a remarkable increase in erosion rates exerted by the surface runoff in many sectors within the fire perimeter, in agreement with literature findings (Moody and Martin 2001; Parise and Cannon 2008, 2012; Staley et al. 2017). Based on the assumption that these processes represent the key aspect governing the availability of sediments to be entrained during rainfalls, and taking into account the available spatial data, the structure of the RUSLE model proved to be the most suitable framework to be adopted. In fact, the approach used is deliberately simple, replicable, improvable and easy to implement in a GIS environment. It is also possible to automate it in order to make it available for the rapid production of thematic maps to support authorities and for civil protection purposes. Moreover, it relies mostly on the available open source spatialized data provided by regional authorities and other public bodies, which makes it easy to replicate the conceptual scheme in other areas. The model has been applied and validated on the Comba delle Foglie catchment, for which a detailed temporal reconstruction of the processes and quantification of the volume of mobilized material has been carried out in a previous work (Vacha et al. 2021).

2 Study Area

The study area is located in the Susa Valley, an east–west Alpine valley, located in the western part of Piedmont (starting ~ 20 km West of Turin). It was affected by the largest and more severe of the ten wildfires that occurred in the region in 2017 (The Bussoleno and Mompantero Wildfire) which burned 4000 ha on the left of the Dora Riparia River, going up the valley from east to west and affecting the slope almost to the divide (Fig. 1). The fire started on October 22, 2017 and lasted until November 1, 2017. It interested an area dominated by European Beech (*Fagus sylvatica L.*) and Scots Pine (*Pinus sylvestris L.*), the forest cover being the 37.1% and the 26.7% for the Broadleaved and the Coniferous species, respectively, with 36.2% of the wildfire surface being represented by non-forested areas (Morresi et al. 2022). Comba delle Foglie is one of the catchments affected by this exceptional wildfire. It is located towards the eastern side of the wildfire area and is a steep, elongated watershed ranging between 480 and 1747 m a.s.l., characterized by an average slope of 35° and an area of approximatively 1.37 km^2 (Vacha et al. 2021). The bedrock

Layout: T3_Color Book ID: 525824_1_En Book ISBN: 978-3-031-16897-0
Chapter No.: 6 Date: 30-9-2022 Time: 5:07 pm Page: 3/14

of the catchment is represented by polimethamorphic rocks and in particular by Micaschists and gneiss belonging to the Dora Maira pre-triassic basement (DMb), by calcschists, marbles and dolomitic marbles belonging to the Dora Maira Mesozoic cover (DMc) and by calcschists, serpentinites, serpentinoschists and chloritoschist belonging to the Lower Piedmont Zone (PZ) (Carraro et al. 2002; Gasco et al. 2011). The geomorphological setting of the study is both influenced by its geologic history and by quaternary geomorphic events. The main valley is dominated by erosional and depositional landforms of glacial origin, mainly glacial terraces, suspended-tributary valleys and lodgement and ablation till. The post-glacial remodeling action exerted by gravitative and fluvial processes strongly influenced the landscape. In particular, the left side of the Susa Valley hosts a series of ravine and canyon-like features in correspondence of morphological steps at the outlet of suspended valleys into the main valley. As a result, the quaternary deposits mantle the study area heterogeneously: the main valley floor is filled by alluvial deposits, while the slope are patched by glacial, fluvial and gravity related deposits, often reworked (Cadoppi et al. 2007).

The vegetative cover of the catchment before the fire was low with respect to other sectors of the burned area due to previous wildfires (Ascoli et al. 2011), and it was mostly dominated by young trees of *Populus tremula* and *Salix caprea*. The most relevant parameters describing the watershed are given in Table 1, in which the major morphometric descriptors can be found.

3 Materials and Methods

3.1 Burn Severity

The burn severity map of the Bussoleno and Mompantero Wildfire (Morresi et al. 2022) was adopted in this work. This map was produced through satellite imagery and field surveys, following a methodology based on US FIREMON framework (Key and Benson 2005). The analysis of spectral changes caused by the 2017 wildfires was carried out using multispectral images acquired by the MultiSpectral Instrument (MSI) onboard Sentinel-2 A/B satellites (European Space Agency). In particular, the burn severity obtained by using the uncalibrated RdNBR bi-temporal index (Miller and Thode 2007, Eq. 1) calculated from reflectance composites was adopted here. It was generated using all the clear observations available in the period spanning from 20 May to 10 September for both 2017 and 2018; the validation of the map and the classification in severity categories followed Miller et al. (2009), Miller and Thode (2007) and Parks et al. (2014). This product was chosen because among all the other indices calculated by the authors, it was the one with the best overall accuracy.

$$RdNBR = \frac{dNBR}{\sqrt{|NBR_{prefire}|}} \quad (1)$$

RdNBR is based on the definition of the Normalized Burn Ratio (NBR) (Eq. 2) which is calculated by contrasting the

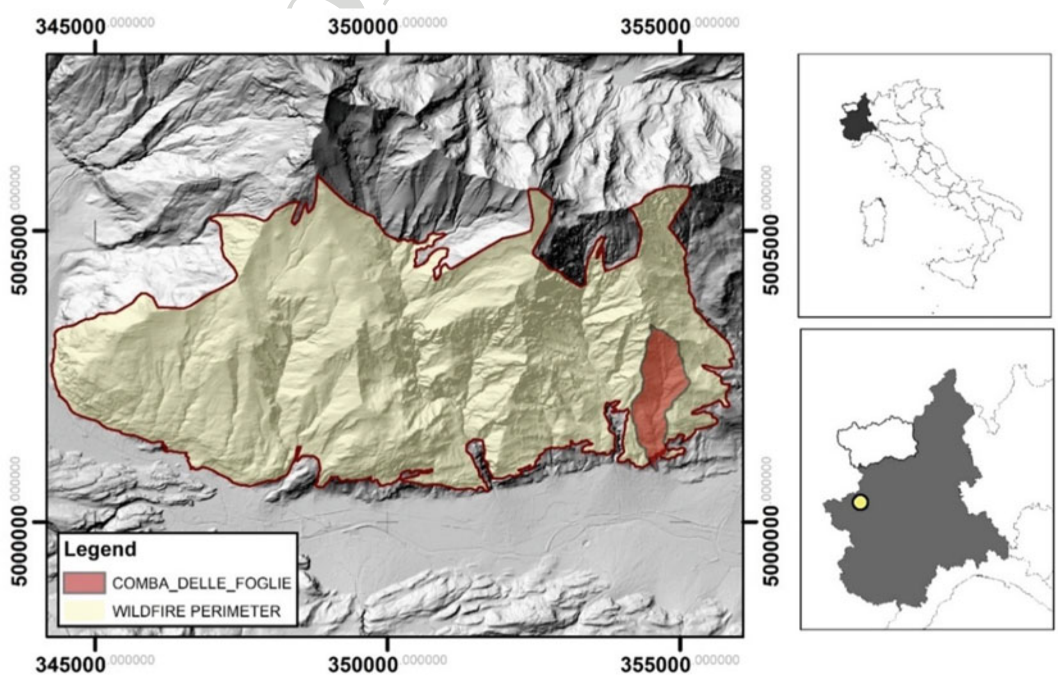

Fig. 1 Perimeter of the Susa valley wildfire and location of the Comba delle Foglie watershed. The base map is the regional DTM

Table 1 Morphometrical and hydrological descriptors of the Comba delle Foglie watershed; area Aw [km^2], perimeter P [km], watershed length Lb [km], minimum elevation Emin [m s.l.m.], maximum elevation Emax [m s.l.m.], mean elevation Emea [m s.l.m.], minimum slope Smin [°], maximum slope Smax [°], mean slope Smea [°], main channel length Lp [km], average main channel slope LpS [°], total streams length L [km], Fan to watershed area ratio Af_Aw [−], Form factor Ff [−] (Horton 1932), Circularity ratio Rc [−] (Miller 1953; Strahler 1964), Elongation ratio Re [−] (Schumm 1956), Melton Index Me [−] (Melton 1965), Drainage density Dd [km/km^2] (Strahler 1964), Time of concentration Tc [h] (Kirpich 1940)

Index	Unit	Value	Index	Unit	Value	Index	Unit	Value
Aw	[km^2]	1.37	Smax	[°]	74.82	Af_Aw	[−]	8.14
P	[km]	6.1	Smea	[°]	35.01	Ff	[−]	0.22
Lb	[km]	2.59	Lp	[km]	2.44	Rc	[−]	0.44
Emin	[m a.s.l.]	480	LpS	[°]	32.22	Re	[−]	0.53
Emax	[m a.s.l.]	1747	L	[km]	4.14	Me	[−]	1.02
Emean	[m a.s.l.]	1035				Dd	[km/km^2]	3.19
Smin	[°]	1.5				Tc	[h]	0.18

reflectance in the near infrared (NIR) and in the shortwave infrared (SWIR); the delta Normalized Burn Ratio (Key and Benson 2006) is calculated through Eq. (3).

$$NBR = [(NIR - SWIR)/(NIR + SWIR)] \quad (2)$$

$$dNBR = \left(NBR_{prefire} - NBR_{postfire}\right) \times 1000 \quad (3)$$

RUSLE—Monthly erosion calculation

Sediment erosion has been assessed implementing the RUSLE model at a monthly scale through the following equation:

$$A_{month} = R_{month} * K * L * S * C * P \quad (4)$$

where A = mean soil loss per month [Mg ha^{-1} m^{-1}], R = rainfall erosivity factor [MJ mm h^{-1} ha^{-1} m^{-1}], K = soil erodibility factor [Mg MJ^{-1} mm^{-1} h], LS = topographic factor or slope length factor [dimensionless], C = soil coverage [dimensionless], and P = erosion control practices factor [dimensionless]. The value of the sediment loss (SL) is obtained by multiplying the value of A for the drainage surface. The R factor quantifies the mechanical impact energy exerted by a given precipitation and depends on duration and intensity of the rainfall. Remaining parameters in the equation give a measure of the environmental resistance to erosive phenomena. The K, LS and C factors are assumed to change in areas affected by wildfires as a result of fire effect on soil erodibility, vegetative cover and shift in rill to interrill soil erodibility ratio (Terranova et al. 2009). RUSLE model is intended to quantify soil losses in the long term, so that processes such as gully and channel erosion and sediment transport cannot be modelled. Prediction accuracy for individual storm is very low, as controversial is the application on large spatial scale. Despite this, the model can be used as a solid framework to quantify high-risk erodible areas (Efthimiou et al. 2020). With this regard, the product of K, LS and C factor is used to compare post-fire to pre-fire condition; thus, EI [Mg MJ^{-1} mm^{-}1 h] is introduced to describe the erosion susceptibility:

$$EI = C * K * Ls \quad (5)$$

P factor has been considered equal to 1, because there are no support practices for the erosion reduction in the study area.

Rainfall erosivity factor—R

The rainfall erosivity factor (R) factor has been estimated at a monthly scale by calculating the summation of the parameter EI_{30} of every single erosive event (k) for each considered month.

$$R_{month} = \sum_{k=1}^{n} EI_{30k} \quad (6)$$

Following Brown and Foster (1987), EI_{30} for a single rainstorm event is defined as the product of the kinetic energy of rainfall events (E) and its maximum 30-min intensity (I_{30}):

$$EI_{30} = \left(\sum_{r=1}^{m} e_r v_r\right) I_{30} \quad (7)$$

where e_r = unit rainfall energy [MJ ha^{-1} mm^{-1}], v_r = rainfall volume [mm] during the r-th period of a storm which divided into m parts and I_{30} is the maximum 30-min rainfall intensity [mm h^{-1}]. The unit rainfall energy e_r is calculated for each time interval using Eq. (8) (Brown and Foster, 1987):

$$e_r = 0.29\left[1 - 0.72e^{(-0.05 i_r)}\right] \quad (8)$$

Layout: T3_Color Book ID: 525824_1_En Book ISBN: 978-3-031-16897-0
Chapter No.: 6 Date: 30-9-2022 Time: 5:07 pm Page: 5/14

Table 2 Location of the three rain gauges of Prarotto, Borgone and Malciaussia

Name	Elevation (m s.l.m.)	WGS84-UTM32N X (m)	WGS84-UTM32N Y (m)	Basin
Prarotto	1440	361,493	5,000,737	Dora riparia
Borgone	400	361,958	4,997,582	Dora riparia
Malciaussia	1800	354,590	5,007,700	Stura di lanzo

where i_r is the rainfall intensity during the time interval [mm h^{-1}]. High resolution rainfall data (10 min time resolution) were downloaded from Arpa Piemonte database for three rain gauges located in the surrounding of the watershed, namely Prarotto, Borgone and Malciaussia (Table 2 and Fig. 2). Rainfall series covers a period of time ranging from September 1, 2017 to August 3, 2018. The identification of the erosive rainfall (n) events for each station record followed three criteria given by Renard et al. (1997): the cumulative rainfall of an event is greater than 12.7 mm, or the event has at least one peak that is greater than 6.35 mm during a period of 15 min. Individual storms are separated if a rainfall accumulation is less than 1.27 mm during a period of 6 h. Those criteria have been developed for the USA countries, but are also widely accepted in other areas (Panagos et al. 2015a). The Rainfall Intensity Summarisation Tool (RIST) software (USDA 2014) was used to calculate the R-factor based on the single station annual series. After that, the single monthly R factors related to each rain gauge were averaged to get the final value representative of the watershed. The obtained results were compared with the average monthly rainfall erosivity calculated by Ballabio et al. (2017) at European scale analyzing > 17 years of rainfall data and downloaded from ESDAC repository (European Soil Data Centre, European Commission, Joint Research Centre).

Soil erodibility factor—K

The soil erodibility (K) factor has been determined based on soil textural data. Homogeneous lithological units have been individuated by grouping the geological units derived from 1:50,000 geological map (Carraro et al. 2002). Soil samples have been then collected and processed in laboratory for determining grain size distribution following standard ASTM procedures. Afterwards, the K factor for each unit has been then calculated based on the following formulae (Renard et al. 1997):

$$K = 0.0034 + 0.0405 * \exp\left[-0.5\left(\frac{\log D_g + 1.659}{0.7101}\right)^2\right] \tag{9}$$

$$D_g = \exp\left[\sum f_i \ln\left(\frac{d_i + d_{i-1}}{2}\right)\right] \tag{10}$$

where D_g = geometric mean particle size for each particle size class (clay, silt, sand), d_i = maximum diameter (mm), d_{i-1} = minimum diameter and fi is the corresponding mass fraction.

Cover factor—C

The C factor has been assessed based on Forestry/Land Cover Map and by assigning C values according to Panagos et al. (2015b). Tabulated values for each land cover class are given in Table 3, whilst land cover classes areal distribution is given in Table 4.

Length/Slope Factor LS

The LS factor in the original RUSLE model describes the interaction between standard parcel length (L) and slope (S). In this study, it is substituted by the unit contributing area Ls, which takes into account the flow convergence (Mitasova et al. 1996; Terranova et al. 2009). Ls is computed for each 5 m wide DTM cell as follows:

$$Ls = (\mu + 1)(a/a_0)^{\mu}(\sin b/b_0)^{\eta} \tag{11}$$

where a [m] = the upslope contributing area for each cell (result of the ArcGIS "flowacc" and "resolution" functions), b [%] = slope, a_0 [m] = 21.1 m (the standard USLE plot length), and b_o [%] = 9% (the standard USLE plot slope). The parameter μ is calculated as a function of β, which is the ratio of rill to interrill erosion (Miller et al. 2003; Foster et al. 2003):

$$\mu = \beta/((1 + \beta)) \tag{12}$$

Based on literature, β can be set equal to 0.5 for unburned areas and equal to 1 for burned areas with high severity. The parameter η is considered equal to 1.2 following Terranova et al. (2009) and Coschignano et al. (2020). The cell values in a buffer of 10 m around the stream network has been excluded from the calculation since the RUSLE model does not provide estimates for streamflow erosion. For them, a default value of 0 has been assigned.

Model implementation

Pre-fire monthly mean soil loss (A_{pre}) and erodibility index (EI_{pre}) were calculated based on the previous equations on a 5 m resolution raster grid based on DTM cells position.

Layout: T3_Color Book ID: 525824_1_En Book ISBN: 978-3-031-16897-0
Chapter No.: 6 Date: 30-9-2022 Time: 5:07 pm Page: 6/14

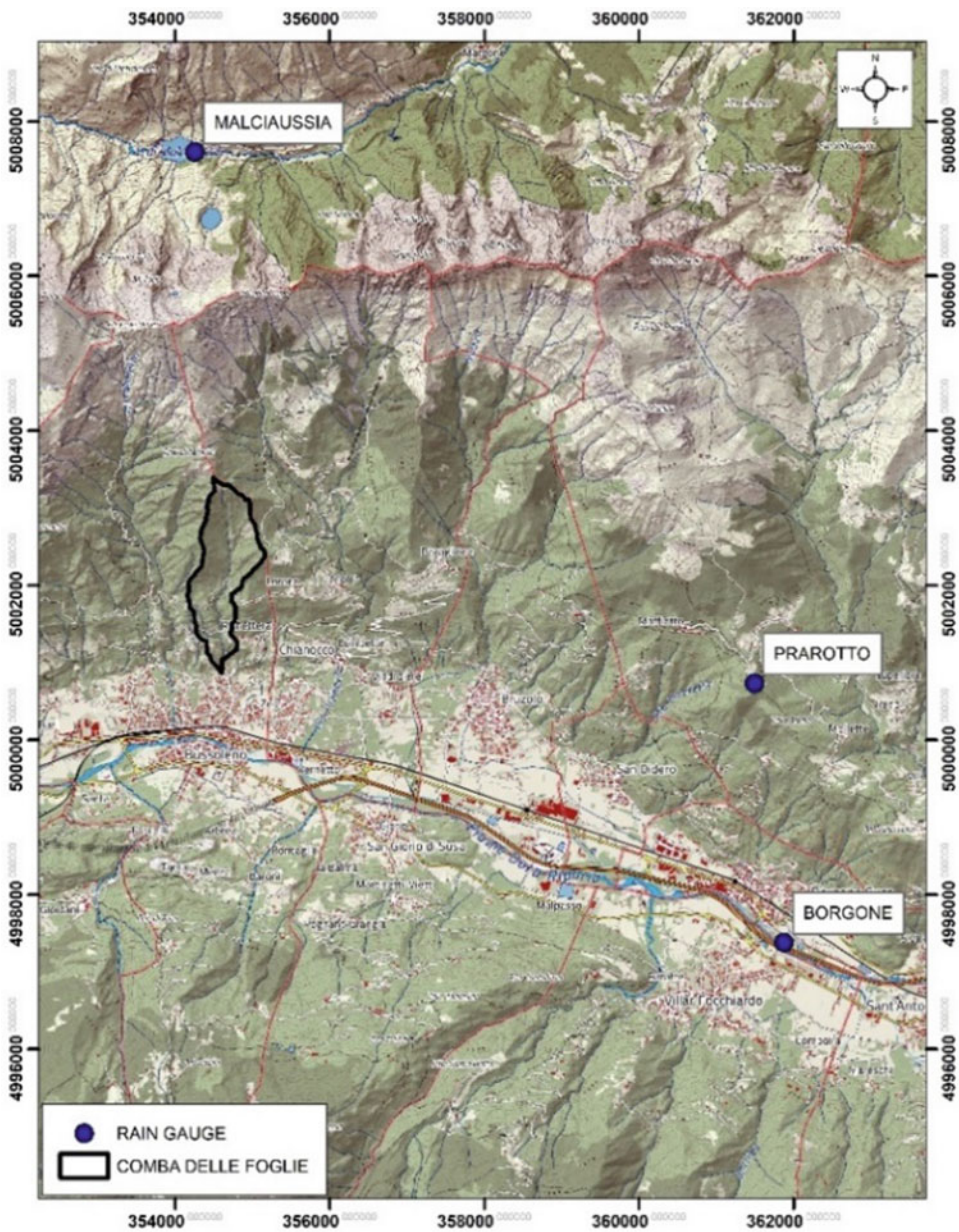

Fig. 2 Location of the three rain gauges of Prarotto, Borgone and Malciaussia with respect to the Comba delle Foglie watershed position

Then the spatially weighted average of A_{w_pre} was calculated over the entire watershed surface.

Finally, the value of the monthly sediment loss (SL_{pre}) [Mg y^{-1}] for the watershed was calculated multiplying the value of A_{w_pre} times the watershed area. Post-fire condition was modeled by calculating mean soil loss per month (A_{post}) and erodibility index (EI_{post}) following Eqs. (3) and (4). The single factors of the RUSLE model were adjusted as a function of fire severity (unburned, low, moderate or high) following with some modifications the procedures described in Terranova et al. (2009) and Lanorte et al. (2019). The metrics used in this work are given in Table 5. For both scenarios (pre- vs post-fire), A and EI raster cell values have been subsequently averaged for each watershed giving $A_{w\text{-}post}$ and SL_{post} value.

4 Results

The fire severity class distribution over the watershed (Fig. 3) highlight a predominancy (77.10%) of moderate fire severity, while unburned/low and high severity cover the 21.98%, and 0.92% of the watershed area, respectively. Given the fact that the area experienced another fire in 2003, the burn severity map may underestimate the 2017 situation, even if a relativized index such as RdNBR has been used.

Table 3 RUSLE cover factor proposed for each land cover class (after Panagos et al. 2015b)

CLC class	Class name	C-factor values	CLC class	Class name	C-factor values
112	Discontinuous urban fabric	0	313	Mixed forest	0.0013
131	Mineral extraction sites	0	313b	Mixed forest < 20%	0.003
211	Non-irrigated arable land	0.23	3211	Natural grassland prevailingly without trees and shrubs	0.04
221	Vineyards	0.34	3212	Natural grassland with trees and shrubs	0.03
222	Fruit trees and berry plantations	0.1	322	Moors and heathland	0.055
231	Pastures	0.09	322b	Moors and heathland	0.055
242	Complex cultivation patterns	0.147	324	Transitional woodland-shrub	0.024
243	Land principally used for agriculture, with significant areas of natural vegetation	0.124	332	Bare rocks	0
311	Broad-leaved forest	0.0013	333	Sparsely vegetated areas	0.25
311b	Broad-leaved forest < 20%	0.003	0	Bare Soil	1
312	Coniferous forest	0.0013			
312b	Coniferous forest < 20%	0.003			

Table 4 Land cover classes areal distribution over the Comba delle Foglie watershed

Land principally used for agriculture	Broad-leaved forest	Mixed forest	Transitional woodland-shrub	Broad-leaved forest < 20%	Mixed forest < 20%	Natural grassland with trees and shrubs
%	%	%	%	%	%	%
5.5	24.5	38.2	4.2	0.6	26.1	0.9

Table 5 Adjusted cover factors (C), erodibility factors (K) and β value (used for LS factor calculation) (β) for different fire severity classes

Burn Severity class	RUSLE parameters		
	C	**K**	**β**
Unburned/Low	C_{pre}	K_{pre}	0.5
Moderate	$C_{pre} + 0.1$	$1.8 * K_{pre}$	1
High	$C_{pre} + 0.25$	$2 * K_{pre}$	1

Monthly R factors for each rain gauge from September 2017 to August 2018 have been quantified by calculating the summation of the parameter EI_{30} of every single erosive event for each considered month. The R factor obtained for each station has been then averaged for assessing the representative rainfall erosive power at the watershed scale. For the Prarotto, Borgone and Malciaussia rain gauges 22, 24 and 22 erosive events, respectively, have been identified. For the Prarotto rain gauge, the selected storms are characterized by a mean precipitation value of 30.94 mm, duration of 23.23 h and EI30 of 95.99 MJ mm ha^{-1} h^{-1}. For the Borgone rain gauge mean precipitation, duration and EI30 values are 27.67 mm, 20.19 h and 73.06 MJ mm ha^{-1} h^{-1}. At the Malciaussia station, mean value recorded are 29.20 mm, 16.02 h and 55.40 MJ mm ha^{-1} h^{-1}, for precipitation, duration and EI30. The maximum values of R factor are reached in May, April and March 2018, and are, on the contrary, equal to zero for September and October 2017.

R factor distribution over time is consistent with Piedmont meteorological data (Arpa Piemonte 2018a, b, 2019), reporting an extremely dry end of 2017 and very wet month of January, April and May 2018. In fact, erosive events registered in these months represents approximatively the 75% of the entire annual R factor, and in particular the month of May reaching almost the 40%. Erodibility K factor representative of the pre-fire condition has been determined based on soil textural data collected during the field surveys.

The pre-fire K values have been calculated following Eqs. (9) and (10). The post-fire adjusted K values have been then calculated by applying the correction procedure described in Table 5. Pre-fire and post-fire K values are reported in Fig. 4 (a, b). Pre-fire c factor (Fig. 4c) has been calculated following the procedure described above, by using the values reported in Table 3; post-fire c factor (Fig. 4d) has been then calculated as given in Table 5. Pre-fire LS factor has been calculated through Eqs. (11) and (12), while post-fire LS values have been calculated through Eq. 12 and Table 5. Results are reported in Fig. 4e, f. P value has been set equal to 1.

Erodibility index values for the pre-fire and post-fire situation (Table 6) has been calculated following Eq. (5), and

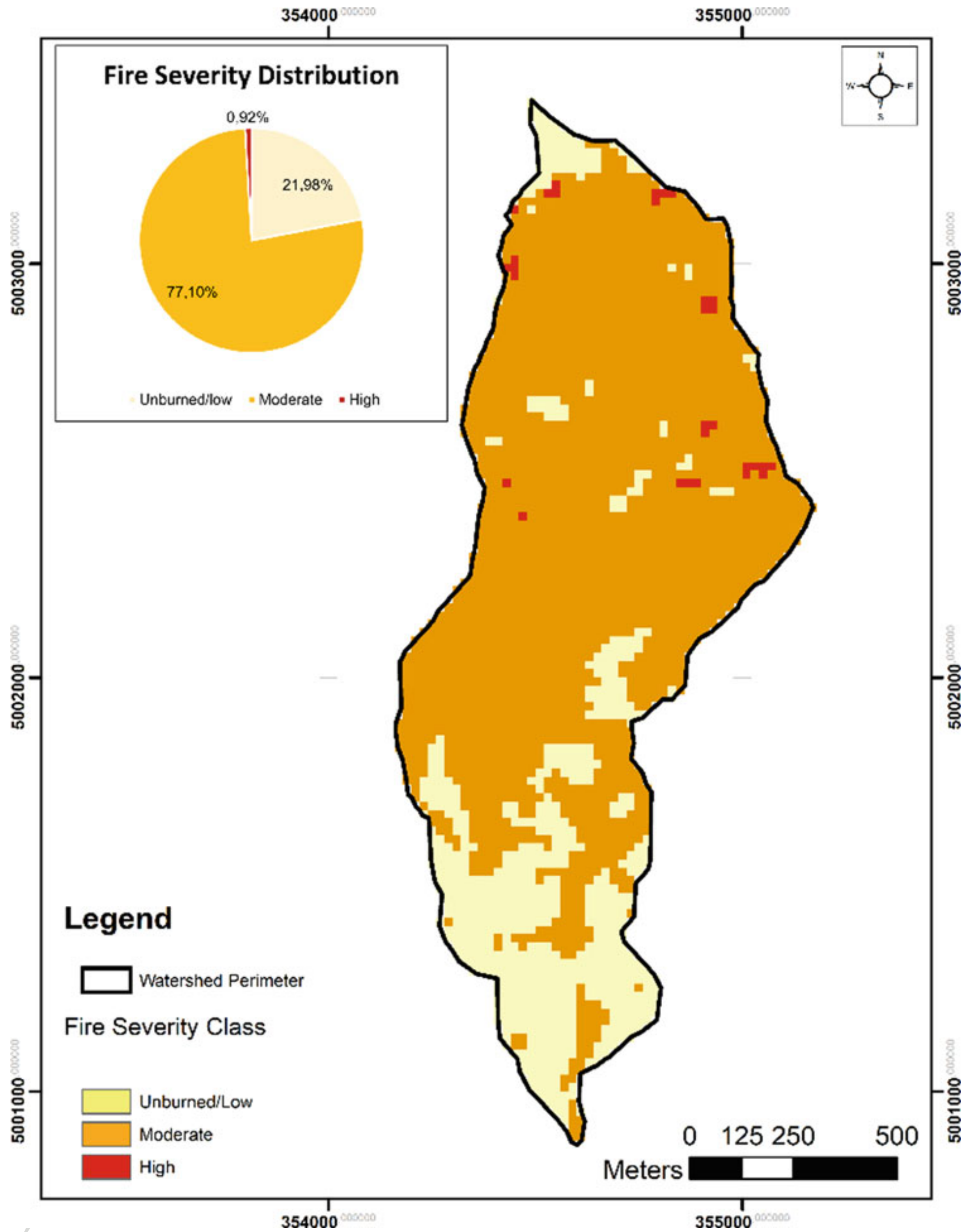

Fig. 3 Fire severity classes distribution for the Comba delle Foglie catchment

finally monthly mean soil loss A [Mg ha^{-1} m^{-1}] and averaged monthly sediment loss SL [Mg m^{-1}] for the entire watershed have been computed for both the burned and unburned condition. The post-fire mean erodibility index is more than one order of magnitude higher than the pre-fire one, having a pre-fire value of 4.63E-04 Mg MJ^{-1} mm^{-1} h and a post fire value of 1.21E-02 Mg MJ^{-1} mm^{-1} h. Also, the maximum values show a rise of about the same order.

Monthly mean soil loss A [Mg ha^{-1} m^{-1}] and averaged monthly sediment loss SL [Mg m^{-1}] comparison for the pre- and post-fire conditions (Fig. 5, Table 7) results in a post-fire increase of both the indicators of more than 20 times with respect to pre-fire. Maximum pre-fire values occur in May, being 0.307 Mg ha^{-1} m^{-1} and 39.86 Mg m^{-1} for monthly mean soil loss and monthly sediment loss, respectively; for the post-fire, these parameters reach values of 8.066 Mg ha^{-1} m-1 and 1050.400 Mg m^{-1}, respectively.

5 Discussion

The sediment erosion has been assessed for the Comba delle Foglie watershed by implementing the RUSLE model at a monthly scale, including model inputs of a detailed erodibility map, the forestry/land cover map, the LS factor map derived from GIS elaboration and a R factor value calculated

Layout: T3_Color Book ID: 525824_1_En Book ISBN: 978-3-031-16897-0
Chapter No.: 6 Date: 30-9-2022 Time: 5:07 pm Page: 9/14

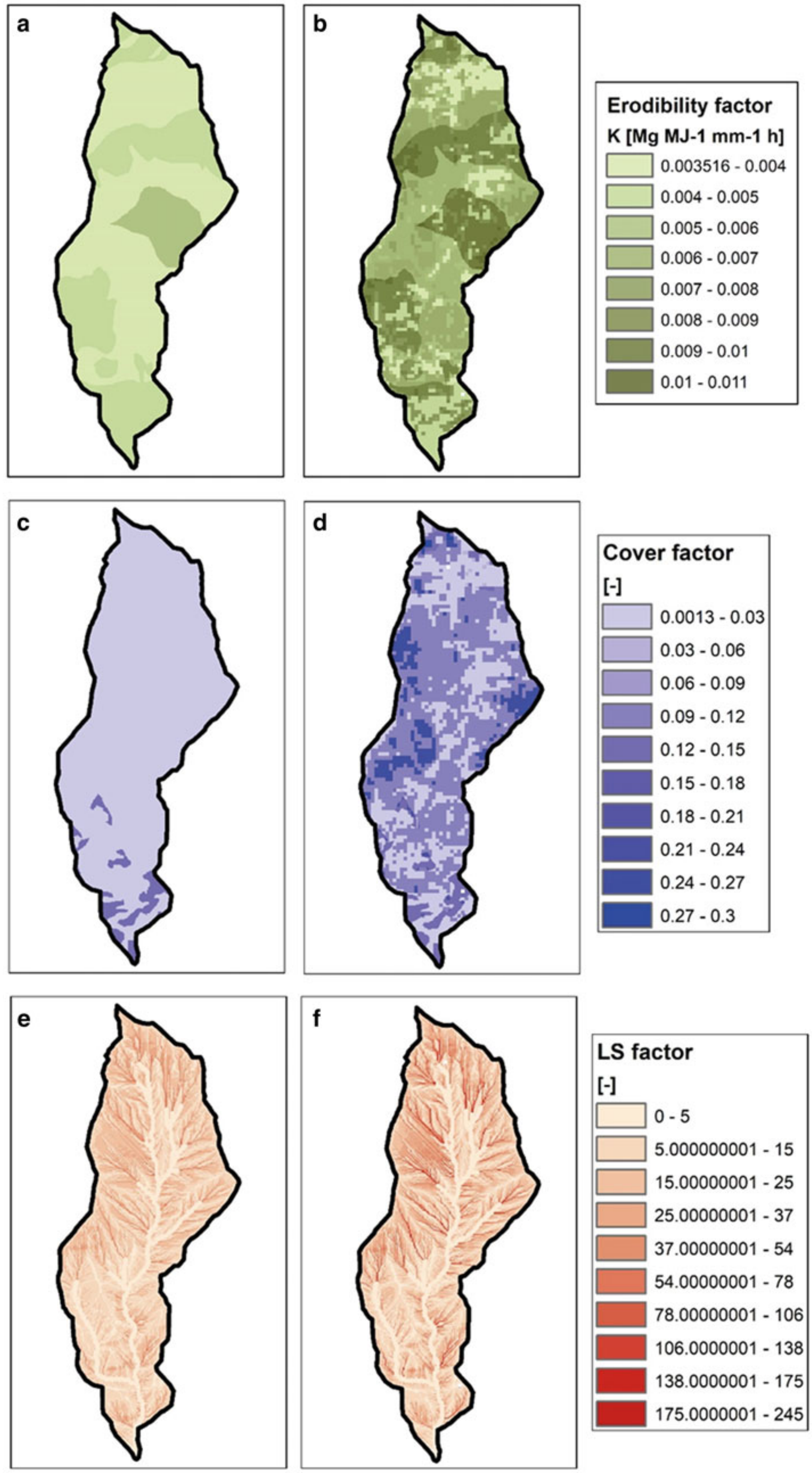

Fig. 4 RUSLE factors distribution over the catchment: pre-fire erodibility factor **a**, post-fire erodibility **b**, pre-fire cover factor **c**, post-fire cover factor **d**, pre-fire LS factor **e** and post-fire LS factor **f**

Table 6 Post-fire versus pre-fire erodibility index values over the Comba delle Foglie watershed

EI [Mg MJ^{-1} mm^{-1} h]	Pre-fire	Post-fire
MIN	0.00E + 00	0.00E + 00
MAX	2.83E - 02	3.54E - 01
MEAN	4.63E - 04	1.22E - 02
STD	1.65E - 03	2.16E - 02

by retrieving the erosive power of every significant rainfall event. Monthly mean soil loss [Mg ha^{-1} m^{-1}] and averaged monthly sediment loss [Mg m^{-1}] are the result of the remarkably R values recorded in the months of January, April and May; these three months in fact contribute for about 75% to the annual erosion recorded in the watershed.

Comparing the calculated R factors to average monthly R factor by Ballabio et al (2017) (Fig. 6) is evident a concentration of the erosive events in the post-fire time window, while the precipitations remained well below the average values from September to December 2017, barely reaching the 6% of the cumulated average value. The months of January, April and May show values eleven, eight and four times greater, respectively, than the long time series data. The RUSLE model estimates a SL of approximatively 2430 Mg from the extinction of the fire to June (included), when the most significant event occurred. To validate this result, the only available information is related to the characterization of the 7 June event: in that case, the maximum deposit thickness of the debris-flow reconstructed via photogrammetric modelling was approximatively 2 m and the invasion area covered about 26,000 m^2. The total mobilized volume for only the coarser fraction of the deposit, was about 4300 m^3, of which about 1500 m^3 consisting of materials entrained just at the fan apex. The volume of the coarser sediments coming from the watershed was estimated to be 1300 m^3. By applying a simple rule of thumb, considering a bulk density of 1500 kg/m^3, the 7 June flow mass can be estimated in 1950 Mg. Considering the fact that other four minor events (one debris/mud flow in April and three floods in May) happened before the 7 June, it is reasonable to presume that the remnant part of the total sediment loss estimated by the model could be related to those events. Some non-negligible aspects undermine the model robustness and accuracy: in fact, the 7 June event volume estimated via photogrammetrical modeling contrast with the one suggested by Arpa Piemonte (2018b) , which after expeditive surveys estimates the total event volume to be about 20,000 m^3. Another aspect which should be taken into account when dealing with the model validation is the remarkable erosion exerted by the debris-flows along all their paths, which may have increased their volumes considerably. The results of the model are not suitable to predict streamflow erosion, so when the estimated value is compared to the available surveyed data, this aspect may also increase the uncertainty. Finally, the current model does not take into account the ash and combustion residues which, for sure, contribute to the overall sediment availability to be entrained. Ash and combustion residues are expected to constitute a large part of the removable material especially immediately after the fire, and that they will then be gradually washed away by the runoff as the rainy events occur. Despite all the model limitations and the uncertainties related to its validation, the presented procedure can be considered a reasonable estimator of the amount of material ready to be eroded during the rainstorm events and conveyed in the riverbeds. In fact, it is backed up by ground evidence, the assumption that the considerable amount of sediment mobilized from the date of the fire have been progressively delivered towards the bottom of the slopes and inside the stream network on the repeated rainfalls. In occasion of some smaller mud-flows and hyper-concentrated flows have originated. Then, when the progressive increase of sediments reached a critical threshold in conjunction with a rainy event of a sustained intensity, the most destructive debris-flow on 7 June occurred. During the field inspections prior to 7 June a considerable amount of sediments and combustion residues had been observed inside the channels, especially in the terminal part of the watershed and at the apex of the fan. The investigations carried out following the event revealed evident traces of areal and channeled erosion, starting from the upper part of the slopes and into the lower-order channels. It is clear how all this mass of sediments, both coming from open slopes and being deposited in the drainage network, has constituted the load of the debris-flow during its transit, simultaneously increasing its energy.

6 Conclusions

The Piedmont region, and in particular the western Italian Alps, experienced an unusually severe wildfire season in 2017. The fires occurred in the late autumn and, after a snowy winter, were followed by spring rains. In particular, some of the catchments burned in the Susa Valley wildfire were interested in May and June 2018 by debris/mud-flows and flood type events. The major debris-flow happened at the outlet of Comba delle Foglie and struck the Bussoleno municipality. Based on field evidence, it was found that the flows mobilized materials and sediments, which were eroded from the burned hillslopes and subsequently deposited in the channels. This is consistent with the literature which reported the main cause of the post-fire debris-flows to be the generation of increased erosion due to excess runoff rather than a discrete landslide failure. On the back of these findings, a modified version of the RUSLE model was applied in

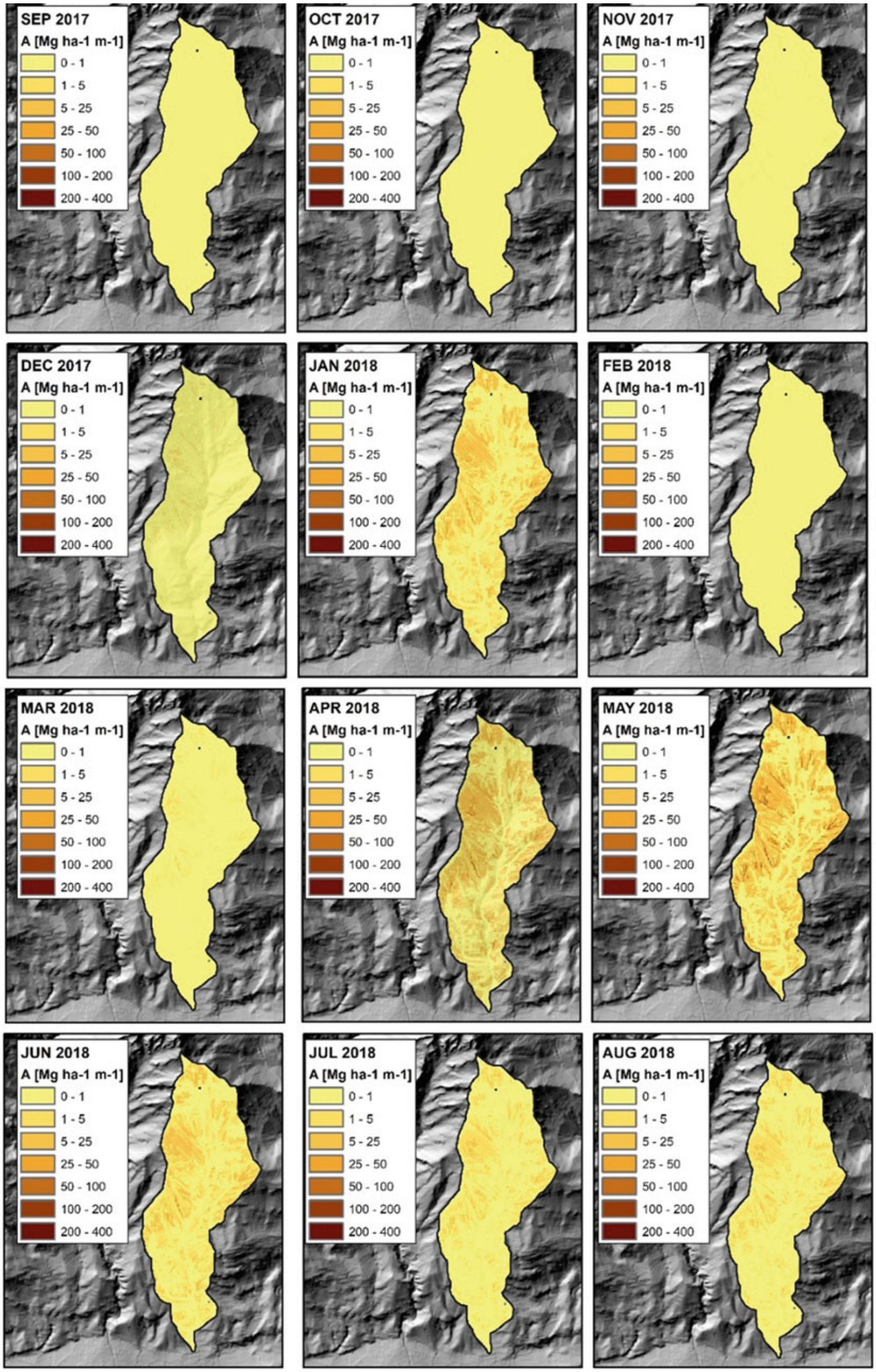

Fig. 5 Monthly mean soil loss

Table 7 Spatially averaged mean soil loss (A) and averaged monthly sediment loss (SL) comparison for the burned and unburned situation

Month	Burned		Unburned	
	A	SL	A	SL
	[Mg/ha*m]	[Mg/m]	[Mg/ha*m]	[Mg/m]
9–17	0.000	0.00	0.000	0.00
10–17	0.000	0.00	0.000	0.00
11–17	0.133	17.32	0.005	0.66
12–17	0.208	27.07	0.008	1.03
1–18	3.342	434.36	0.127	16.48
2–18	0.014	1.82	0.001	0.07
3–18	0.310	40.28	0.012	1.53
4–18	4.223	548.87	0.160	20.83
5–18	8.081	1050.28	0.307	39.86
6–18	2.371	308.14	0.090	11.69
7–18	0.981	127.55	0.037	4.84
8–18	1.014	131.75	0.038	5.00
TOT	20.677	2687.45	0.785	101.98

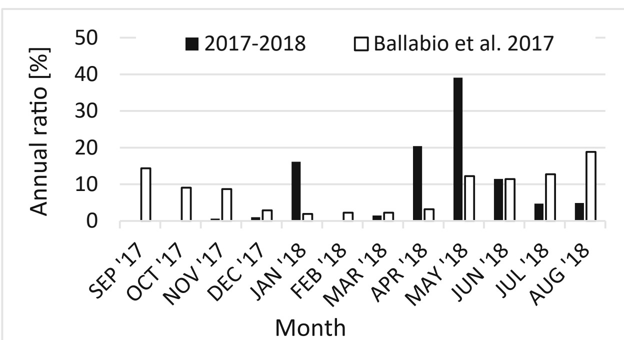

Fig. 6 Comparison between calculated and long term inter annual R-factor (Ballabio et al. 2017)

the area of Comba delle Foglie to quantify the erosive processes on a monthly scale. The results of its application, incorporating high resolution rainfall series and data deriving from field surveys, made it possible to reproduce and highlight the marked increase in erosion rates, quantified by expressing both the EI (erodibility index), the A (monthly soil loss) and the SL (monthly sediment loss) rise. In particular, overall A and SL increased more than twenty times in the post-fire scenario, the months of April, May and June representing the larger share of the total quantities. This is a consequence of the noticeable increase of t EI, which for the post-fire scenario is more than one order of magnitude higher than the pre-fire one. The intrinsic uncertainties of the model are related to the fact that it does not consider the stream-flow erosion in the channels, it does not account for the material eroded by the debris-flow during its passage and it does not incorporate the eroded volume of ash and combustion residues. Some uncertainties are then linked to the fact that the estimates regarding the actual volumes of the flows are limited to a single case (the major one, 7th June) and also do not agree with each other. Despite these uncertainties, the proposed procedure can be considered a reasonable estimator of the amount of material ready to be eroded, especially if it is used to compare different catchments in a relative way; in this case, it can provide useful guidance to rank the post-fire debris-flow susceptibility and to establish intervention priorities. It can be applied everywhere on the regional territory because the model make use on open-source spatialized data and thanks to its structure, it can be easily implemented into a GIS for thematic map production.

Acknowledgements This study is conducted within the ICL IPL project No. 4938. Many thanks to Arpa Piemonte for rainfall data. Field survey were conducted in the framework of the Institutional Technical Table on Wildfire Emergency of the Piedmont Region.

References

Arndt N, Vacik H, Koch V, Arpaci A, Gossow H (2013) Modeling human-caused forest fire ignition for assessing forest fire danger in Austria. Iforest 6:315–325

Arpa Piemonte (2017) Rapporto tecnico sulla qualità dell'aria e sulle attività dell'agenzia a supporto dell'emergenza per gli incendi boschivi in Piemonte nel mese di ottobre 2017

Arpa Piemonte (2018a) Rapporto evento del 07/06/2018, Colata detritica nel comune di Bussoleno

Arpa Piemonte (2018b) Il Clima in Piemonte 2017. Available online at https://www.arpa.piemonte.it

Arpa Piemonte (2019) Il Clima in Piemonte 2018. Available online at https://www.arpa.piemonte.it

Ascoli D, Valsecchi C, Bovio G and Conedera M (2011) Wildfires and beech forests of Southern Alps during the summer 2003 climate anomaly: fire effects and post-fire management. The 5th international wildland fire conference, Sun City, South Africa, 9–13 May 2011

Ballabio C, Borrelli P, Spinoni J, Meusburger K, Michaelides S, Beguería S, Klik A, Petan S, Janecek M, Olsen P, Aalto J, Lakatos M, Rymszewicz A, Dumitrescu A, Tadić MP, Nazzareno D, Kostalova J, Rousseva S, Banasik KL, Alewell C, Panagos P (2017) Mapping monthly rainfall erosivity in Europe. Sci Total Environ 579:1298–1315

Barbero R, Curt T, Ganteaume A, Maillé E, Jappiot M, Bellet A (2019) Simulating the effects of weather and climate on large wildfires in France. Nat Hazards Earth Syst Sci 19:441–454

Bo M, Mercalli L, Pognant F, Cat Berro D, Clerico M (2020) Urban air pollution, climate change and wildfires: the case study of an extended forest fire episode in northern Italy favoured by drought and warm weather conditions. Energy Rep 6:781–786

Brown LC, Foster GR (1987) Storm erosivity using idealized intensity distributions. Trans Am Soc Agric Eng 30:379–386

Cadoppi P, Giardino M, Perrone G, Tallone SD (2007) Litho-structural control, morphotectonics, and deep-seated gravitational deformations in the evolution of Alpine relief: a case study in the lower Susa Valley (Italian Western Alps). Quatern Int 171:143–159

Carabella C, Miccadei E, Paglia G, Sciarra N (2019) Post-wildfire landslide hazard assessment: the case of the 2017 montagna del morrone fire (central apennines, Italy). Geosciences 9:175

Carraro F, Cadoppi P, Baggio P, Bellino L, Castelletto M, Giraud V, Mensio L (2002) Foglio 154 – Susa – Carta Geologica d'Italia, scala 1:50.000. Carta Geol—Serv Geol D'Italia Coord CARRARO F 126

Coschignano G, Nicolaci A, Ferrari E, Cruscomagno F and Iovino F (2019) Evaluation of hydrological and erosive effects at the basin scale in relation to the severity of forest fires. iForest 12:427–434

De Graff JV (2014) Improvement in quantifying debris flow risk for post-wildfire emergency response. Geoenviron Disasters 1:5

Depountis N, Michalopoulou M, Kavoura K, Nikolakopoulos K, Sabatakakis N (2020) Estimating soil erosion rate changes in areas affected by wildfires. ISPRS Int J Geo-Inf 9:562

Dupire S, Curt T, Bigot S, Fréjaville T (2019) Vulnerability of forest ecosystems to fire in the French Alps. Eur J For Res 138:813–830

Efthimiou N, Psomiadis E, Panagos P (2020) Fire severity and soil erosion susceptibility mapping using multi-temporal earth observation data: the case of Mati fatal wildfire in Eastern Attica, Greece. Catena 187(2020):104320

Esposito G, Esposito E, Matano F, Molisso F, Sacchi M, Porfido S (2013) Effects of a wildfire on rocks and soils in the Sarno Mountains, Campania, Southern Apennines. Rend Online Soc Geol Ital 24:119–121

Esposito G, Matano F, Molisso F, Ruoppolo G, Di Benedetto A, Sacchi M (2017) Post-fire erosion response in a watershed mantled by volcaniclastic deposits, Sarno Mountains, Southern Italy. CATENA 152:227–241

Esposito G, Parodi A, Lagasio M, Masi R, Nanni G, Russo F, Alfano S, Giannatiempo G (2019) Characterizing consecutive flooding events after the 2017 Mt. Salto Wildfires (Southern Italy): Hazard and emergency management implications. Water 11:2663

Esteves TCJ, Kirkby MJ, Shakesby RA, Ferreira AJD, Soares J, Irvine B, Ferreira CSS, Coehlo COA, Bento CPM, Carreira M (2012) Mitigating land degradation caused by wildfire: application of the PESERA model to fire-affected sites in central Portugal. Geoderma 191:40–50

Fernandez C, Vega JA (2018) Evaluation of the RUSLE and disturbed wepp erosion models for predicting soil loss in the first year after wildfire in NW Spain. Environ Res 165:279–285

Fernandez C, Vega JA, Vieira DCS (2010) Assessing soil erosion after fire and rehabilitation treatments in NW Spain: performance of RUSLE and revised Morgan–Morgan–Finney models. Land Degrad Dev 21:58–67

Foster GR, Toy TJ, Renard KG (2003) Comparison of the USLE, RUSLE1.06c, and RUSLE2 for application to highly disturbed lands. Proceedings of the first interagency conference on research in the watersheds. USDA—Agricultural Research Service, Washington, DC, pp 154–160

Gasco I, Gattiglio M, Borghi A (2011) Lithostratigraphic setting and P-T metamorphic evolution for the Dora Maira Massif along the Piedmont Zone boundary (middle Susa Valley, NW Alps). Int J Earth Sci 100:1065–1085

Horton RE (1932) Drainage-basin characteristics. EOS Trans Am Geophys Union 13:350–361

IPCC (2014a) Synthesis report. In: Core Writing Team, Pachauri RK, Meyer LA (eds) Climate change 2014. Contribution of working groups I, II and III to the fifth assessment report of the intergovernmental panel on climate change. IPCC, Geneva

IPCC (2014b) Climate change 2014: impacts adaptation and vulnerability. Part A. Global and sectoral aspects. In: Field CB, Barros VR, Dokken DJ, Mach KJ, and others (eds) Contribution of working group II to the fifth assessment report of the intergovernmental panel on climate change. Cambridge University Press, Cambridge

Key CH, Benson NC (2006) Landscape assessment (LA): sampling and analysis methods. In: Lutes D, Keane RE, Caratti JF, Key CH, Benson NC, Sutherland S, Gangi L (eds) Firemon: fire effects monitoring and inventory system. RMRS-GTR-164; Rocky Mountain Research Station, US Department of Agriculture, Forest Service: Fort Collins, CO, USA, 2006; pp LA-1–LA-51

Kirpich ZP (1940) Time of concentration of small agricultural watersheds. Civ Eng 10(6):362

Lanorte A, Cillis G, Calamita G, Nolè G, Pilogallo A, Tucci B, Santis F (2019) Integrated approach of RUSLE, GIS and ESA Sentinel-2 satellite data for post-fire soil erosion assessment in Basilicata region (Southern Italy). Geomat Nat Haz Risk 10(1):1563–1595

Mantero G, Morresi D, Marzano R, Motta R, Mladenoff DJ, Garbarino M (2020) The influence of land abandonment on forest disturbance regimes: a global review. Landscape Ecol 35:2723–2744. https://doi.org/10.1007/s10980-020-01147-w

Maringer J, Ascoli D, Dorren L, Bebi P, Conedera M (2016) Temporal trends in the protective capacity of burnt beech forests (*Fagus sylvatica L.*) against rockfall. Eur J For Res 135(4):657–673

Melton MA (1965) The geomorphic and paleoclimatic significance of alluvial deposits in Southern Arizona. J Geol 73:1–38

Miller JD, Thode AE (2007) Quantifying burn severity in a heterogeneous landscape with a relative version of the delta normalized burn ratio (dNBR). Remote Sens Environ 109:66–80

Miller JD, Nyhan JW, Yool SR (2003) Modeling potential erosion due to the Cerro Grande fire with a GIS-based implementation of the revised universal soil loss equation. Int J Wildland Fire 12:85–100

Miller VCA (1953) Quantitative geomorphic study of drainage basin characteristics in the Clinch Mountain area Virginia and tennessee. Columbia University Technology Report No. 3, Contract N6 ONR, pp 271–30

Mitasova H, Hofierka J, Zlocha M, Iverson LR (1996) Modeling topographic potential for erosion and deposition using GIS. Int J Geogr Inf Sci 10(5):629–641

Moody JA, Martin PA (2001) Initial hydrologic and geomorphic response following a wildfire in the Colorado front range. Earth Surf Proc Land 26:1049–1070

Moreira F, Viedma O, Arianoutsou M, Curt T, Koutsias N, Rigolot E, Barbati A, Corona P, Vaz P, Xanthopoulos G, Mouillot F, Bilgili E (2011) Landscape - wildfire interactions in southern Europe: implications for landscape management. J Environ Manage 92:2389–2402

Morresi D, Marzano R, Lingua E, Motta R, Garbarino M (2022) Mapping burn severity in the western Italian Alps through phenologically coherent reflectance composites derived from Sentinel-2 imagery. Remote Sens Environ 269:112800

Panagos P, Ballabio C, Borrelli P, Meusburger K, Klik A, Rousseva S, Tadic MP, Michaelides S, Hrabalíková M, Olsen P, Aalto J, Lakatos M, Rymszewicz A, Dumitrescu A, Beguería S, Alewell C (2015a) Rainfall erosivity in Europe. Sci Total Environ 511:801–814

Panagos P, Borrelli P, Meusburger K, Alewell C, Lugato E, Montanarella L (2015b) Estimating the soil erosion cover-management factor at the European scale. Land Use Policy 48(2015):38–50

Parise M, Cannon SH (2008) The effects of wildfires on erosion and debris-flow generation in Mediterranean climatic areas: a first database. Proceedings of 1st world landslide forum. Tokyo, Japan, pp 465–468

Parise M, Cannon SH (2012) Wildfire impacts on the processes that generate debris flows in Burned Watersheds: Natural Hazards, vol 61

Parks SA, Dillon GK, Miller C (2014) A new metric for quantifying burn severity: the relativized burn ratio. Remote Sens 6:1827–1844

Renard KG, Foster GR, Weesies GA, McCool DK, Yoder DC (1997) Predicting soil erosion by water: a guide to conservation planning with the revised universal soil loss equation (RUSLE) (Agricultural handbook 703). US Department of Agriculture, Washington, DC, p 404

Rulli MC, Offeddu L, Santini M (2013) Modeling post-fire water erosion mitigation strategies. Hydrol Earth Syst Sci 17:2323–2337

Schumm SA (1956) Evolution of drainage systems and slopes in badlands at Perth Amboy. New Jersey, Geol Soc Am Bull 67:597–646

Sheridan GJ, Lane PN, Smith H, Nyman P (2009) A rapid risk assessment procedure for post-fire hydrologic hazards; 2009/10 fire season. Technical report produced for the department of sustainability and environment. The Department of Forest and Ecosystem Science, The University of Melbourne, Australia, p 19. ISBN 9780734041470

Staley DM, Negri JA, Kean JW, Laber JL, Tillery AC, Youberg AM (2017) Prediction of spatially explicit rainfall intensity–duration thresholds for post-fire debris-flow generation in the Western United States. Geomorphology 278:149–162

Staley DM, Negri JA, Kean JW, Tillery AC, Youberg AM (2016) Updated logistic regression equations for the calculation of post-fire debris-flow likelihood in the western United States: U.S. Geological Survey Open-File Report 2016–1106, p 13

Strahler AN (1964) Quantitative geomorphology of drainage basin and channel networks. Handbook of applied hydrology

Tang H, McGuire LA, Rengers FK, Kean JW, Staley DM, Smith JB (2019) Evolution of debris-flow initiation mechanisms and sediment sources during a sequence of postwildfire rainstorms. J Geophys Res Earth Surf 124:1572–1595

Terranova O, Antronico L, Coscarelli R, Iaquinta P (2009) Soil erosion risk scenarios in the Mediterranean environment using RUSLE and GIS: an application model for Calabria (southern Italy). Geomorphology 112(2009):228–245

Tiranti D, Moscariello A, Giudici I, Rabuffetti D, Cremonini R, Campana V, Bosco F, Giardino M (2006) Post-fire rainfall events influence on debris-flows trigger mechanisms, evolution and sedimentary processes: the Rio Casella case study in the North-western Italian Alps. Geophys Res Abstr 8:03479

USDA (2014) United States department of agriculture. Rainfall Intensity Summarization Tool (RIST). Accessed from, http://www.ars.usda.gov

Vacha D, Mandrone G, Garbarino M, Morresi D (2021) First consideration about post 2017 wildfire erosion response and debris flow in Susa Valley (NW Italy). In: Tiwari B, Sassa K, Bobrowsky PT, Takara K (eds) Understanding and reducing landslide disaster risk. WLF 2020. ICL contribution to landslide disaster risk reduction. Springer, Cham

Wastl C, Schunk C, Leuchner M, Pezzatti B, Menzel A (2012) Recent climate change: long-term trends in meteorological forest fire danger in the Alps. Agric for Meteorol 162–163:1–13

Wischmeier WH, Smith DD (1978) Predicting rainfall erosion losses: a guide to conservation planning. Agriculture Handbook no. 537, USDA, Washington DC, USA, pp 13–27

Zumbrunnen T, Bugmann H, Conedera M, Bürgi M (2009) Linking forest fire regimes and climate—a historical analysis in a dry inner Alpine valley. Ecosystems 12:73–86

Author Query Form

Book ID :	**525824_1_En**
Chapter No :	**6**

Please ensure you fill out your response to the queries raised below and return this form along with your corrections.

Dear Author,
During the process of typesetting your chapter, the following queries have arisen. Please check your typeset proof carefully against the queries listed below and mark the necessary changes either directly on the proof/online grid or in the 'Author's response' area provided below

Query Refs.	Details Required	Author's Response
AQ1	References 'Dupire et al. (2019), Thang et al. (2019), Key and Benson (2005)' are cited in the text but not provided in the reference list. Please provide the respective references in the list or delete these citations.	